JOURNAL OF MATERIALS SCIENCE 6 (1971) 281–288

Stress Relaxation in Beryllia

D. G. WALKER, W. B. ROTSEY, B. R. A. WOOD
Materials Division, AAEC Research Establishment, Sutherland, NSW, Australia

Beryllia beams were loaded at temperature in four-point bending to a deflection of 0.001 in. or 0.002 in. and the decrease in load necessary to maintain the deflection constant was measured as a function of time. The beryllia was fine-grained, in the range ~ 1 to 7 μm, and the porosity varied between 3 and 21%. The test conditions covered a temperature range of 850 to 1240°C, experiments took from 10 min to 8 h: the loads used produced initial maximum outer fibre stresses of the order 3000 to 6000 psi.

A method was developed for calculating the stress distribution in a beam at any time and this was used to analyse the results. The stress relaxation process was found to be stress-activated, and the conversion of elastic to plastic strain could be expressed as a creep law having the form

$$\dot{\epsilon} = k_0 \exp\left(\frac{-Q}{RT}\right) \exp\left(\frac{C\nu\sigma}{RT}\right).$$

The activation energy was 100 ± 2 kcal mole^{-1} and the activation volume was large, probably of the order of 10^3 atoms. The rate constant k_0 was approximately proportional to the fraction of intergranular porosity and inversely proportional to the cube of the grain diameter. It is suggested that the mechanism of grain boundary sliding is consistent with the observations.

1. Introduction

In recent years ceramics have become important in the fields of nuclear, aeronautical and space engineering, and this fact has created an interest in their high temperature, time-dependent properties. Work has been reported on the creep of magnesia [1-3], alumina [4] and beryllia [5, 6].

The related phenomenon of stress relaxation has so far received little attention in the study of ceramics, although it has provided much useful information in the study of deformation mechanisms in metals. Not only should such experiments give an insight into ceramic behaviour, but stress relaxation is of considerable technological importance in the engineering application of ceramic components, for example in an environment producing thermal stress.

The lack of any published information on stress relaxation in ceramics is probably due to the experimental difficulties involved. In a relaxation test it is necessary to strain a speicmen and then, keeping the strain constant by continually adjusting the load, to note the decrease in stress as a function of time. Difficulties arise during tests as changes of 1% in the total strain must be sensed and, with ceramics, only a small total strain can usually be imposed before fracture occurs.

Whilst a compression test would have the merit of simplicity, particularly in the calculation of stress, the strain on a 1 in. gauge length would be of the order of 6×10^{-4} in., necessitating the sensing of changes of the order of 6×10^{-6} in. A bend test offered an attractive method of obtaining an increased deflection for the same strain. Unfortunately, interpretation of the data from such experiments can be difficult since the required stress-strain relationship is not directly obtainable from the load-deflection measurements, but depends also on the distribution of stress and strain within the beam. In certain cases, for example elastic deflection in four-point bending, these distributions are known and a simple relation exists between measured and required values; in creep deformation, however, these distributions are complex and generally unknown and simplifying assumptions must be made. It is often assumed that the stress distribution in creep is identical to that for elastic deflection [5]; under certain conditions of creep this

may be an accurate description but in general it leads to significant errors [7]. In the present case it was decided to attempt a more general solution to the problem of relaxation in a beam under four-point bending and to apply this to a study of stress relaxation in BeO.

2. Stress Relaxation in a Bent Beam

It must be possible to relate the behaviour of a material undergoing creep to that occurring during relaxation since both involve the same time-dependent process of deformation, provided that during relaxation the decrease in stress does not change the mechanism of deformation. Given an equation describing this time-dependent process, in principle it is possible to deduce the strain-time relation for creep or the stress-time relation for relaxation. For example, we can assume an equation of the form

$$\dot{\epsilon}_{\text{creep}} = f_1(T) f_2(\sigma) f_3(t)$$

since in relaxation the total strain ϵ remains constant, and

$$\epsilon = \epsilon_{\text{elastic}} + \epsilon_{\text{creep}}$$

It then follows that

$$\dot{\epsilon}_{\text{creep}} = -\dot{\epsilon}_{\text{elastic}} = -\frac{1}{E}\frac{\mathrm{d}\sigma}{\mathrm{d}t}$$

and the stress-time relation at constant temperature can be obtained by integration,

$$\int_{\sigma 0}^{\sigma 1} \frac{\mathrm{d}\sigma}{f_2(\sigma)} = -f_1(T) E \int_0^{t1} f_3(t)\,\mathrm{d}t \qquad (1)$$

In simple tension or compression experiments, the measured load-time data are related directly to the required stress-time function, but in the case of the bent beam the relation is more complicated.

Provided that the behaviour in tension and that in compression are equivalent, the neutral axis will remain in the centre of the beam. If the beam is considered to be made up of a number of thin slabs parallel to the neutral axis then each slab approximates to an element in simple tension or compression. Since the total strain in each element remains constant, the relaxation process can be imagined to occur independently in each slab, hence the beam can be treated as a series of independent tensile (and compressive) elements relaxing from an initial stress set by the position of the element relative to the neutral axis. For a distance y from the neutral axis this will be given by

$$\sigma = \frac{My}{I}$$

where M is the bending moment and I is the section modulus.

Given any particular creep law, equation 1 can be solved for each element in the beam and the stress-time relations can be determined. Thus for any particular time, the stress in every element may be computed and the stress distribution across the beam obtained. From this, integration gives the bending moment,

$$M = 2b \int_0^{h/2} \sigma y\,\mathrm{d}y$$

where h is the depth of the beam and b is the width, and from the geometry of the apparatus, the load supported at that instant may be calculated. Repeating these steps allows a load-time curve to be synthesised.

In practice, a high speed digital computer is used to synthesise a series of load-time curves corresponding to a series of possible creep equations. These curves are then compared with the experimental data and the one giving the best fit is selected.

The above model for relaxation in a bent beam has a corollary: the shape of the beam remains constant throughout the relaxation. The small strains used in the present experiments did not allow for accurate measurement of shape change, but profile measurements were carried out on a beryllia bar bent to large deflections under creep conditions at similar temperatures; these measurements showed that the shape was the same as that under elastic deflection to within a few per cent. Thus the use of the above model appeared justified.

3. Experimental Materials

Blocks were fabricated from Brush UOX powder which was homogenised by grinding with water for 1 h, dried, and isostatically pressed at 20 tsi; the blocks were then sintered in the range 1400 to 1500° C for various times to give a range of densities. Specimens were machined from the blocks to dimensions of 3.250 × 0.400 × 0.125 in. with tolerances of ± 0.001 in.

Density was determined for each specimen from its mass and physical dimensions. Fractional porosity was calculated as

$$P = \frac{3.01 - \text{density}}{3.01}$$

and values are given in table I.

TABLE I Specimen Parameters

Specimen no.	Porosity P	Grain size d (μm)
1, 2	0.03	7.3
3	0.06	2.3
4	0.11	1.3
5	0.16	1.3
6	0.21	1.1

After the relaxation experiments, each specimen was sectioned, polished, etched and examined by replica electron microscopy. The microstructures were uniform with equiaxed grains except for occasional large needle-shaped grains which are characteristic of this grade of BeO [8]. Porosity was uniformly distributed in the samples of 16% porosity and less, but somewhat segregated in the 21% porous sample. For the samples of 3% porosity, some of the pores were intergranular, whereas for the lower density specimens all pores were at grain boundaries.

Grain sizes (table I) were measured on enlargements of the electron micrographs and are quoted as mean linear intercepts; this allowed for porosity. The large needle-shaped grains were ignored.

4. Experimental Techniques

The specimens rested on beryllia knife edges 3.0 in. apart, and were loaded via upper knife edges 0.75 in. apart. The load was transmitted to the upper knife edge block by means of a ball and tube. The central deflection of the specimen was measured by a linear differential transformer which was capable of detecting changes of $\pm$ 2 μin.

The load was applied by means of a movable weight on a cantilever beam. At the beginning of a test the weight was rapidly run out along the beam thus loading the specimen. When the central deflection of the specimen reached 0.002 in. the output from the deflection-sensing transducer actuated a trip amplifier stopping the movement of the weight. As the specimen crept, the change in deflection was sensed, and when it exceeded 2 μin. the trip amplifier operated to return the weight along the beam until the deflection of the specimen was again 0.002 in. The sensitivity of the device was such that the load could be relaxed in increments of 0.05 lb. The load was measured by a load cell to an accuracy of $\pm$ 0.1 lb. The output from the load cell was fed directly into a conventional recorder so that a load-time curve was obtained automatically.

The accuracy of temperature control required was greater than could be obtained with available controllers. The technique adopted was to operate the specimen furnace at a chosen stabilised voltage, a period of 12 to 24 h being allowed for the system to attain thermal equilibrium. Temperature control of the laboratory was essential and it was kept at 20 $\pm$ 0.5°C.

A specimen was placed in the apparatus and heated at the chosen temperature for at least 12 h to attain thermal equilibrium. A series of relaxation curves were obtained on each specimen, a minimum of 12 h annealing being allowed prior to a relaxation determination at each new temperature.

In most cases a deflection of 0.002 in. was used although a few relaxations were performed at 0.001 in. deflection. Initial loads varied from specimen to specimen but the peak fibre stresses were generally in the range 6000 to 3000 psi.

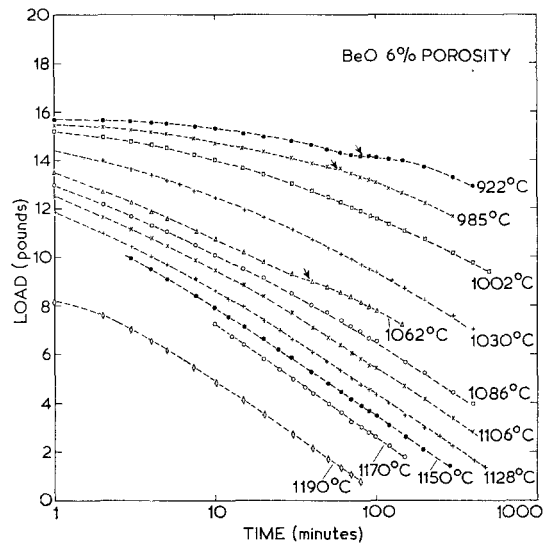

Figure 1 Stress relaxation data for beryllia specimens of 6% porosity. Arrows indicate fluctuations produced by variations in ambient temperature.

5. Results

A typical set of results is shown in fig. 1 in which the load-time data points read from the recorder chart for various temperatures are plotted for the specimen of 6% porosity. The data points generate a family of curves although some deviations are detectable at long times (see arrows in fig. 1).

In all cases such deviations correlated with changes in ambient temperature and the points obtained subsequent to these were therefore ignored.

Similar results were obtained for each of the other specimens and several general conclusions could be drawn.

(*a*) The rate of stress relaxation at any given temperature was very structure sensitive and increased by many orders of magnitude from the highest to the lowest density specimen.

(*b*) For any given specimen, the rate of relaxation increased rapidly with increasing temperature.

(*c*) Above 1062°C the load-time curves were approximately of the form "load proportional to log of time", suggesting that the rate of relaxation was very sensitive to stress.

The computer method described above was applied to derive the creep law governing the observed relaxation. Detailed attention was concentrated on two types of law, the power law for stress

$$\epsilon = f_1(T)\,\sigma^{\beta}\,,$$

and the stress activation law

$$\epsilon = f_1(T)\exp(\alpha\sigma)\,,$$

for various values of the parameters α and β. Initial conditions (σ_0) were calculated from the Young's Modulus measured at room temperature on each experimental bar and published equations for its temperature dependence [10]. Since the computed and observed curves were plottee as load against log (time), one curve for any set of parameter values sufficed for all values of $f_1(T)$. The experimental data were plotted on tracing paper and placed over the computed curves drawn to the same scale. Sliding the trace horizontally allowed the "better fit" value of α or β to be determined and once this was fixed, the values of $f_1(T)$ could be read.

In all cases, the best fit to the experimental curves was obtained for the stress activation law. Fig. 2 shows data from fig. 1 arranged to produce one curve and the "best fit" computed curves for both laws namely

$$\dot{\epsilon} = f_1(T)\,\sigma^{5.5}$$

and

$$\dot{\epsilon} = f_1(T)\exp(2.8 \times 10^{-2}\sigma)\,,\ \sigma \text{ in kg cm}^{-2}\,.$$

It is clear that the agreement for the stress activation case is excellent and is significantly better than for the power law. Fig. 3 shows a similar treatment of the data for the 11% porosity sample. In this case the "best fit" computed curves are

$$\dot{\epsilon} = f_1(T)\,\sigma^{5.0}$$

$$\dot{\epsilon} = f_1(T)\exp(3.7 \times 10^{-2}\,\sigma)\,,\ \sigma \text{ in kg cm}^{-2}\,.$$

The present data cannot be interpreted in terms of a creep law with the first power of the stress ($\beta = 1$ over the stress range in the beam) such as has been suggested from higher temperature creep data [5].

The equations considered above apply to steady state or secondary creep. Transient or primary creep conditions, particularly those described by equations of the form $\dot{\epsilon} = f_1(T)\sigma^{\beta}t^{\gamma}$ were also investigated but gave no significant improvement in fit to the experimental data.

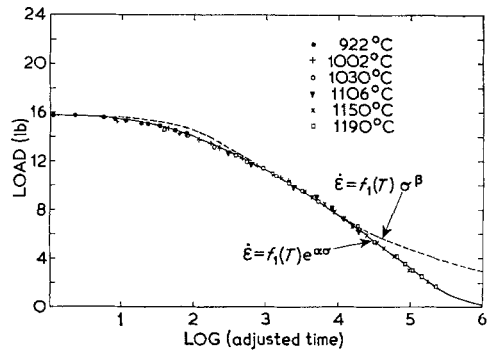

Figure 2 Compound diagram showing data from fig. 1 fitted to a single curve by adjusting the time axis. Also shown are theoretical curves derived from the following creep equations. Curve 1: $\dot{\epsilon} = f_1(T)\sigma^{5.5}$. Curve 2: $\dot{\epsilon} = f_1(T)$ exp($2.8 \times 10^{-2}\,\sigma$), σ in kg cm^{-2}.

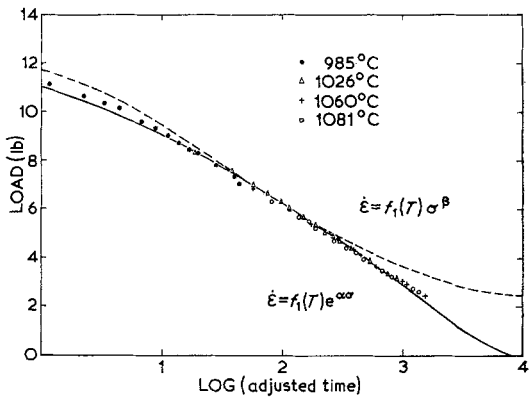

Figure 3 Compound diagram as in fig. 2 but for specimen of 11% porosity. Curve 1: $\dot{\epsilon} = f_1(T)\,\sigma^{5.0}$. Curve 2: $\dot{\epsilon} = f_1(T)$ exp ($3.7 \times 10^{-2}\sigma$), σ in kg cm^{-2}.

Analysis of the data from all the specimens gave the following results for

(*a*) The stress concentration factor (α).

Within the accuracy of measurement ($\pm$ 10%) the values of α determined for any one specimen were independent of temperature. However, there was some variation from specimen to specimen. As the density increased the value of α initially decreased, then rose again at high densities.

(*b*) The temperature dependence $f_1(T)$.

For any one specimen, the values of $f_1(T)$ could be analysed as

$$f_1(T) = k_0 \exp(-\ Q/RT).$$

Within the experimental error, the values of the activation energy (Q) were close to 100 kcal mole^{-1} in each case; indeed, by adjusting the k_0 values all the data could be fitted on a single Arrhenius line as shown in fig. 4. The activation energy over the temperature range 850 to 1250°C determined from this compound diagram was 100 $\pm$ 2 kcal mole^{-1}. The values of k_0 were found to be very dependent on microstructure and a variation of five orders of magnitude was observed for the range of specimens investigated.

The values of α and k_0 for each specimen are given in table II. Some estimate of the reproducibility of the experiment was obtained from specimens 1 and 2 which had nominally identical microstructures and gave results indistinguishable from one another.

6. Discussion

The theory of stress activated processes has been discussed by many authors [10-12]. In brief, in any thermally activated deformation process with activation energy Q, there will be work done by or against the applied stress during this process so that the rate of deformation is given by

$$\dot{\epsilon} = k_0 \exp(-\ Q/RT) \sin h(C\nu\sigma/RT)$$

where k_0 is a frequency factor, ν is a parameter having the dimensions of volume and is referred to as the activation volume, and C is a numerical factor relating the effective stress to the applied stress. For cases where $C\nu\sigma > RT$, the approximation $\sin hx \sim e^x$ may be used, that is,

$$\dot{\epsilon} = k_0 \exp(-\ Q/RT) \exp(C\nu\sigma/RT),$$

or

$$\dot{\epsilon} = k_0 \exp(-\ Q/RT) \exp(\alpha\sigma),$$

where

$$\alpha = C\nu/RT.$$

The significance of the parameters ν, Q and k_0 in the present case will now be discussed.

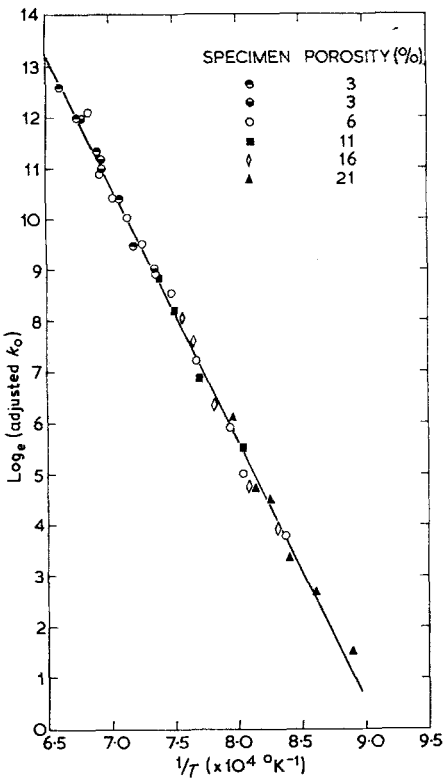

Figure 4 Compound Arrhenius diagram of data from all specimens fitted to a single line by adjusting the frequency factors. Straight line is for activation energy of 100 kcal mole^{-1}.

TABLE II Creep Equation Parameters

Specimen no.	α (cm^2 kg^{-1}) ($\times 10^2$)	k_0 (sec^{-1})	Apparent activation volume $C\nu$ (cm^3 mole^{-1}) ($\times 10^{-3}$)	Apparent activation volume $C\nu$ (Å^3 event^{-1}) ($\times 10^{-3}$)	$k_1 = k_0 d^3 P^{-1}$ (cm^3 sec^{-1}) ($\times 10^{-8}$)
1, 2	3.7	2.8×10^3	4.5	7.5	0.4
3	2.8	1.5×10^6	3.1	5.1	3.0
4	3.7	1.4×10^7	4.1	6.8	2.8
5	4.0	1.8×10^7	4.2	7.0	2.6
6	5.1	2.6×10^8	5.1	8.5	16.0

6.1. The Activation Volume v

The experimental results suggested that α was independent of temperature. Because $\alpha = Cv/RT$ and the stress concentration factor would not be expected to vary appreciably, the activation volume should be proportional to temperature. However, considering the inaccuracies in the determination of α, no significance could be given to this relation. The results show that, unlike the case for stress relaxation in some metals, the activation volume is not highly sensitive to temperature.

Mean values of the apparent activation volume Cv, are given in table II. It is clear that there is some variation with structure although it is not a simple relation with specimen density. At least part of this could arise from the presence of structural irregularities such as pores, since the stress concentration at a pore is a complex function of pore size, shape and distribution. This would mean that the numerical factor C rather than the activation volume would be the structure-sensitive term.

Because the magnitude of the numerical factor is unknown, it is not possible to determine absolute values of the activation volume. However, it is probable that $C < 10$ so that the volume is large compared with that found for metals when associated with dislocation climb, cross slip, or overcoming the Peierls-Nabarro stress.

6.2. Activation Energy Q

The activation energy is large (100 kcal mole^{-1}), but similar values have been observed in creep [5] and sintering [13] experiments in BeO. Most published values of activation energies for cation and anion self-diffusion in BeO fall in the range 50 to 60 kcal mole^{-1} [14-16] however, there is evidence to suggest that these values are associated with impurity effects. Condit and Hashimoto [17] found a change in the activation energy for beryllium self-diffusion from 62 kcal mole^{-1} above 1500°C to 92 kcal mole^{-1} below this temperature.

On the other hand, the process of relaxation may not be controlled by bulk diffusion, but by grain boundary diffusion, as in the case of grain boundary sliding. Measurements of the activation energy of diffusion of beryllium in BeO with porosities varying from 9.8 to 12.8% (very similar to those used in the present work) yielded a result of 139 ± 20 kcal mol^{-1} [18]. No corresponding results appear to be available for oxygen. Nevertheless the observed activation energy of 100 kcal mole^{-1} for the relaxation process possibly means that the controlling mechanism is the diffusion of beryllium ions along grain boundaries.

6.3 Frequency Factor (k_0)

It is evident from the data of table II that the frequency factor is very sensitive to microstructure. Two microstructural parameters which could be expected to influence the frequency factor are porosity and grain size. Assuming that a relation exists of the form.

$$k_0 = k_1 d^m P^n ,$$

where d is the grain size and P the porosity, the closest fit is obtained for $m = -3$ and $n = 1$; this is illustrated in table II. The agreement is excellent for porosities from 16 to 6%, and variations at either end are not unexpected since segregation of porosity at 21% was observed in the microstructure. A change from grain boundary to intragranular pores was found for the denser specimens.

It now remains to consider these parameters in relation to possible mechanisms of the relaxation process.

6.4. The Relaxation Mechanism

Before discussing possible mechanisms for the observed relaxation, it is important to stress that in these experiments the deformation was occurring at relatively low temperatures, in the range 0.4 to 0.5 T_m. Although the hexagonal crystal form of BeO does not persist to the melting point [19], the phase change which occurs before melting appears to be of the martensitic type and therefore does not demand a high diffusivity for its propagation. Thus, in this system, the melting temperature is a more relevant reference point than the phase transition temperature. Hence at a temperature of only 0.4 T_m, those processes which require large numbers of point defects produced by thermal activation such as Nabarro-Herring [20, 21] and Coble [22] creep will not be favoured and, indeed, the stress dependence found in the present experiments is inconsistent with such models.

The present results require a model which predicts a large activation volume and a large activation energy. Considering the range of creep mechanisms which have been proposed for metals, the one which is closest to these requirements is for creep controlled by the glide of jogged

dislocations [10]. However, the application of this model in the present case raises serious problems. Although slip deformation of BeO single crystals has been observed at temperatures around 1000°C, it occurs only under high resolved shear stresses (5000 psi at 1600°C) and is exclusively basal slip [23]. Thus, even if the stress concentration at microstructural defects were sufficient to induce basal slip in the present experiments, some other deformation mechanism must also occur to maintain grain boundary coherence. Further, with a model of this type, it is difficult to explain the observed kind of structure sensitivity in the frequency factor.

Eliminating both diffusional and dislocation mechanisms leaves only deformation by grain boundary sliding. Gifkins and Snowden [24] have proposed a model for creep by grain boundary sliding in which the mechanism is controlled by diffusion from tensile to compressive ledges. In addition, the problem of accommodation at triple points by diffusional creep along the grain boundary at the triple point has been fully discussed by Gifkins [25]. He has also [26] carried out a detailed comparison of creep mechanisms controlled by diffusion, in which sliding theories are compared with creep caused by diffusion through the grains (Nabarro-Herring) and through grain boundaries (Coble).

Recently, creep has been shown to occur in polycrystalline MgO without measurable grain strain [27], implying grain boundary sliding. Unfortunately, the strains achieved in the present experiments were too small to allow significant measurement of grain strain, but it seems possible that grain boundary sliding could predominate in the relaxation of BeO.

Current models for the diffusion control of grain boundary sliding involve atom-by-atom processes so that the corresponding activation volume is the atomic volume. However, the above results require that a relatively large amount of deformation occurs during a single activation process; such a situation would arise if the sliding was not continuous during the transfer of an atom plane around a ledge but was held up until the last atom was transferred. Such a process satisfies the conditions imposed by the parameters but it is difficult to justify physically and the present information is insufficient to support further speculation.

The rate of sliding depends on the volume fraction of material which is subjected to high local stress. Pores are stress-concentrating features and the fraction of grain boundary area under the influence of the pores is roughly proportional to the porosity. If the controlling diffusion process is grain boundary transport, the creep rate will be inversely proportional to the cube of the grain size. In the samples with 6, 11 and 16% porosity, most of the triple points were occupied by pores (see fig. 5) and this may be expected to facilitate accommodation at the triple points. In accordance with the propositions above, the results are reasonably represented by an equation of the form

$$\dot{\epsilon} = k_1 P/d^3 \exp(-Q/RT) \exp(C\nu\sigma/RT) .$$

Clearly this model is not unique and there are too many uncertainties in the data to allow a useful estimation of the constant k_1. However, it appears that a mechanism involving grain boundary sliding, with diffusion control and "equilibrium" boundary configurations separated by many atoms, is required to explain the observed stress relaxation in beryllium oxide.

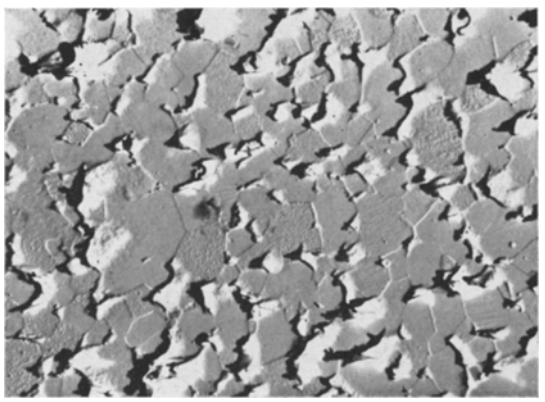

Figure 5 Electron micrograph of 16% porous beryllia × 20000.

7. Conclusions

1) At stresses of less than 6000 psi and at temperatures below 0.5 T_m, stress relaxation in beryllia does not proceed by a simple Nabarro-Herring type mechanism, but is stress-activated. The conversion of elastic to plastic strain follows a creep law of the form

$$\dot{\epsilon} = k_1 P/d^3 \exp(-Q/RT) \exp(C\nu\sigma/RT) .$$

2) The activation energy of the process is 100 ± 2 kcal/mole, and the activation volume is large, probably of the order of 10^3 atoms.

3) It is suggested that the predominant mechan-

ism of the relaxation process is grain boundary sliding.

Acknowledgements

The authors wish to thank Dr R. J. C. Brown for advice on the computer solutions, and Dr R. C. Gifkins for helpful discussions.

References

1. T. VASILOS, J. B. MITCHELL, and R. M. SPRIGGS, *J. Amer. Ceram. Soc.* **47** (1964) 203.
2. E. M. PASSMORE, R. H. DUFF, and T. VASILOS, *ibid* **49** (1966) 594.
3. J. H. HENSLER and G. V. CULLEN, *ibid* **51** (1968) 557.
4. E. M. PASSMORE and T. VASILOS, *ibid* **49** (1966) 166.
5. W. L. BARMORE and R. R. VANDERVOORT, *ibid* **48** (1965) 499.
6. R. E. FRYXELL and B. A. CHANDLER, *ibid* **47** (1964) 283.
7. S. TIMOSHENKO, 'Strength of Materials', Vol. 2, Third Edition (Nostrand Co., New York, 1956) pp. 530-533.
8. T. E. CLARE, *J. Nucl. Mat.* **14** (1964) 359.
9. First Annual Report, High Temperature Materials and Reactor Component Development Programs Vol. 1, Materials (1962). GEMP, 106A, p. 85.
10. H. CONRAD, *J. Metals* (July, 1964) 582.
11. R. E. REED-HILL and E. P. DAHLBERG, *Trans. AIME* **236** (1966) 679.
12. P. FELTHAM, *Philosophical Magazine* **6** (1961) 259.
13. M. J. BANNISTER, *J. Nucl. Mat.* **10** (1964) 315.
14. H. J. DE BRUIN and C. M. WATSON, *ibid* **10** (1964) 239.
15. J. BIRCH-HOLT, *ibid* **11** (1964) 17.
16. S. B. AUSTERMAN, R. A. MEYER, and D. G. SWARTHOUT, *NAA-SR*-6427 (1961).
17. R. H. CONDIT and Y. HASHIMOTO. *J. Amer. Ceram. Soc.* **50** (1967) 425.
18. H. J. DE BRUIN, private communication.
19. J. B. CONWAY and R. A. HEIN, *Nucleonics* **22** (6) (1964) 71.
20. F. R. N. NABARRO, Report of a Conference on the Strength of Solids, The Physical Society (London, 1948), p. 75.
21. C. HERRING, *J. Appl. Phys.* **21** (1950) 437.
22. R. L. COBLE, *ibid* **34** (1963) 1679.
23. G. G. BENTLE and R. N. KNIEFEL, referred to by S. C. Carniglia in 'Materials Science Research', Vol. 3, edited by W. W. Kriegel and H. Palmour, p. 425-471.
24. R. C. GIFKINS and K. U. SNOWDEN, *Trans. AIME* **239** (1967) 910.
25. R. C. GIFKINS, *J. Inst. Metals.* **95** (1967) 373-377.
26. *Idem, J. Amer. Ceram. Soc.* **51** (1968) 69.
27. J. H. HENSLER and G. V. CULLEN, *ibid* **50** (1967) 587.

Received 24 February 1969 and accepted 4 January 1971.